Plasma/Particle Interaction in Subsonic Argon/Helium Thermal Plasma Jets

W. D. Swank
J. R. Fincke
D. C. Haggard
Idaho National Engineering Laboratory
E G & G Idaho, Inc.
Idaho Falls, Idaho

EGG-M--92454
DE93 010808

Abstract

Understanding the behavior of a particle and the interactions between a particle and the plasma surrounding it is important to the development and optimization of the plasma spray coating process. This is an experimental study of the interaction between a subsonic thermal plasma jet and injected nickel-aluminum particles. The velocity, temperature and composition of the gas flow field is mapped using an enthalpy probe/mass spectrometer system. The particle flow field is examined by simultaneously measuring the in-flight size, velocity, and temperature of individual particles. The complex interaction between the gas and particle flow fields is examined by combining the two sets of data. Particle and gas temperatures and velocities are compared in the vicinity of a nominal substrate standoff distance and axially along the median particle trajectory. The temperature and velocity difference is shown to vary substantially depending on the particle's trajectory. By the time a particle on the median trajectory reaches the nominal substrate stand off of 63.5 mm it is transferring it's heat and momentum to the plasma gas.

THE PLASMA FLOW FIELD OF AN ATMOSPHERIC spray process is characterized by it's temperature, velocity, enthalpy, and specie concentration. Temperatures in the plasma are too high for the application of traditional techniques such as thermocouples and uncooled pitot tubes, and often are not high enough for application of emission spectroscopy techniques. While sophisticated laser techniques have been developed and applied to these types of flow fields, they are expensive and require delicate, complicated equipment.[1,2,3] In many situations the application of thermodynamic probes to the measurement of local gas characteristics represents a robust, low cost alternative. The enthalpy probe is considered to be a reliable diagnostic tool in the range from 2000 to 14000 K [4,5,6] and has been used in high temperature flow field research since the 1960's. More recently the enthalpy probe has been rediscovered and is enjoying wide application to a variety of thermal plasma processing problems.[7,8,9] The measurement system used here integrates a differentially pumped quadrapole mass spectrometer with the fully automated enthalpy probe. Complete maps of the argon-helium plasma gas flow field issuing into stagnant laboratory air have been made between axial positions of 5 and 100 mm.

These maps of the gas flow field describe the environment the particles are subjected to upon injection. The particle flow field is characterized by the particle size, velocity, temperature and number density. The in-flight coincidence technique that integrates a two color particle temperature measurement with an absolute magnitude of scattered laser light particle size measurement and a laser Doppler velocimeter has been previously described[10]. The particle measurements presented here where made utilizing these techniques. They are Eulerian, i.e. a spatial description, therefore it is impossible to follow the history of an individual particle. However, for the purposes of studying particle/gas interactions, the gas flow field maps have been overlaid with the particle flow field measurements. Particle/gas temperature and velocity differences are presented along with a comparison of how the environment for a particle following the median trajectory differs from that of one following the geometric center line of the torch and gas flow field. Results from the

plasma spraying of Ni-Al powder, a common adhesion coating, are presented.

Measurement Techniques

The plasma velocity, temperature and composition are obtained from the combination of an enthalpy probe and mass spectrometer. This system has been discussed elsewhere[11], hence only a brief description is included here. The enthalpy probe is a water jacketed gas sampling and stagnation pressure probe from which the enthalpy, temperature, and velocity of a hot flowing gas can be derived once the composition is known. The probe is fabricated from three concentric tubes. The outer tube is copper and has an outside diameter of 4.8 mm. The inner most tube is also copper and has an inside diameter of 0.78 mm.

The calorimetric method used to determine gas enthalpy and hence temperature depends heavily on a "tare" measurement, which effectively eliminates errors in the cooling water temperature measurements. Observations of the coolant temperature rise and flow rate are made while no gas flows through the inner diameter of the probe. Gas is then allowed to flow and the same coolant measurements are repeated, together with measurements of the gas flow rate and gas temperature at the probe exit. The rate of heat removal from the gas sample is thus given by the difference between the measured delta of cooling water inlet and outlet temperatures,

$$\dot{m}_g(h_{1g}-h_{2g}) = \dot{m}_{cw}C_p[(\Delta T_{cw})_{gas\ flow} - (\Delta T_{cw})_{no\ gas\ flow}] \quad (1)$$

where m_g = gas sample mass flow rate, m_{cw} = cooling water mass flow rate, h_{1g} = unknown gas enthalpy at the probe entrance, h_{2g} = gas enthalpy at the probe exit thermocouple, C_p = cooling water specific heat, and ΔT_{cw} = cooling water temperature rise. The unknown gas enthalpy h_{1g} at the probe tip is now uniquely determined, provided that the gas sample flow rate m_g and the gas enthalpy h_{2g} at the probe exit are known. The exit gas enthalpy is determined from the measured temperature at atmospheric pressure and the gas sample flow rate is measured via a sonic orifice.

While in the "no gas flow" portion of the measurement the probe behaves like a water cooled pitot tube and the stagnation pressure can be determined at it's tip. Then for low Mach numbers the free stream velocity, V, of the hot gas may be calculated from,

$$V = \left[\frac{2}{\rho}(P_{stag} - P_{atm})\right]^{\frac{1}{2}} \quad (2)$$

where ρ is the mixture density.

Thermodynamic properties such as density, enthalpy, etc. are determined from a free-energy minimization calculation of complex chemical equilibrium composition[12]. To accurately calculate these properties the composition of the gas must be accurately known. To this end we have integrated a mass spectrometer with the enthalpy probe system. During the "gas flow" phase of the measurement, a gas sample is bled off to a quadrapole mass spectrometer or residual gas analyzer (RGA) (Leybold-Heraeus Inficon Quadrex 100) which is set up in a differentially pumped vacuum system.

The Residual Gas Analyzer is the most difficult and critical portion of the system to calibrate. A linear regression between known mixtures of gasses and measured values is used to supply the calibration which accounts for mass discrimination, ionization efficiency and transmission characteristics of the analyzer. The limitations of the mass spectrometer and the largest source of error resides in the resolution of its 8 bit digitizer. This resolution error is minimized by optimizing the operating voltage of the electron multiplier and by adjusting the individual mass channel electronic gains until a reasonable sensitivity is achieved. Optimizing the gain in this way results in an uncertainty of 10% in the air fraction measurement, when the air fraction is in the neighborhood of 0.2, and a similar uncertainty in the argon to helium ratio under the same conditions. Using standard techniques[13] the estimated 2σ uncertainty in measured enthalpy is 5.3% with the major source of error being the determination of the gas mass flow rate through the probe. This error stems from the inaccuracy of the thermocouple temperature measurement up stream of the sonic orifice. At high temperatures (6000+ K) moderate changes in the enthalpy of the gas mixture produce small changes in the gas temperature. It is for this reason that the combination of a 10% uncertainty in properties and a 5.3% uncertainty in the measured enthalpy result in an acceptable 2σ uncertainty of 4.9% in the determination of gas temperature. The 2σ uncertainty on velocity is 6.3% and its major source of error is in determining the density of the gas mixture.

The system developed for the simultaneous measurement of particle size, velocity and temperature integrates a crossed beam LDV system with a scattered light particle size measurement and a high speed two-color pyrometer[10]. Physically, the measurement system consists of two sets of optics which are rigidly mounted with the laser to a translation table. The movement of the table results in a precise positioning of the measurement volume relative to the plasma device. The spatial resolution of less than 1 mm^3 makes it possible to map the distribution of particle size, velocity, temperature and number density in typical flow fields.

The two-color pyrometery temperature measurement is calibrated against a standard tungsten ribbon lamp. The temperature of the tungsten ribbon is determined by a disappearing wire pyrometer. The lamp is placed behind a chopper rotating at constant speed to simulate the passage of particles through the measurement volume. The uncertainties in the determination of temperature arise from uncertainties in the calibration coefficients; the gray body assumption; and random fluctuations in the ratio of signal voltages. These in combination lead to an estimated one standard deviation uncertainty in temperature of 125K at 2500K.

Calibration of the particle size measurement is performed against a Berglund-Liu vibrating orifice aerosol generator using methanol as the working fluid. A correction to this calibration, based on Mie scattering theory and published values of the particle's index of refraction, is then generated. Finally, the calibration is checked against actual particles. The estimated one-standard deviation uncertainty in size is 4.9 μm.

In calibrating the laser Doppler velocimeter only the laser wavelength and the angle between the beams is required to establish the relationship between the velocity of the scattering particle and the frequency output of the photodetector. The estimated velocity uncertainty is less than 5%.

Results and Discussion

The plasma torch (Miller SG-100) geometry and general particle flow field characteristics are shown in Figure 1. Nominal torch operating conditions are 800 A at 35 V, for a total power input of 28 kW. At these conditions the torch is 68% efficient. The inlet plasma gas flow rate is 2830 liters/hr of argon and 1330 liters/hr of helium. The particle carrier gas flow rate is 368 liters/hr, also argon. All results were obtained in air at an atmospheric pressure of 85.5 kPa.

A commercially available powder (Alloys International Al-1037) was used for this study. The powder consists of a metal core with a Ni-Al skin that is bonded without the use of an organic binder and has a nominal diameter of 50 to 125 μm. Particles are injected on the diameter of the anode inside the body of the torch. The measured particle injection velocity is 15.0 m/s with a standard deviation of 2.4 m/s. Their initial momentum is transverse to the jet, causing the center line of the particle trajectory to be below the geometric center line of the torch. The Ni-Al spray system is characterized by a non-symmetric spray, significant flow-induced particle sizing and an apparent fracturing or stripping of molten material to form smaller particles[14].

To characterize the plasma gas flow field into which the particles are injected the velocity, temperature and composition have been mapped between axial locations of 5 and 100 mm with the enthalpy probe for the torch operating conditions described above. For obvious reasons the enthalpy probe measurements were performed without particle injection, but include the effect of the particle carrier gas. This raises the question of particle loading effects on the plasma flow field[15,16]. Even at injection rates typical of industrial spraying conditions the particle flow field is quite dilute in concentration (< 1000 cm^{-1}) and volume fraction ($< 3 \times 10^{-5}$). Although the mass fraction is significant (approx. 30%) compared to the mass flow rate of gas , the energy and momentum extracted from the plasma that goes into particle heating, melting, and acceleration is less than 5 percent of the total

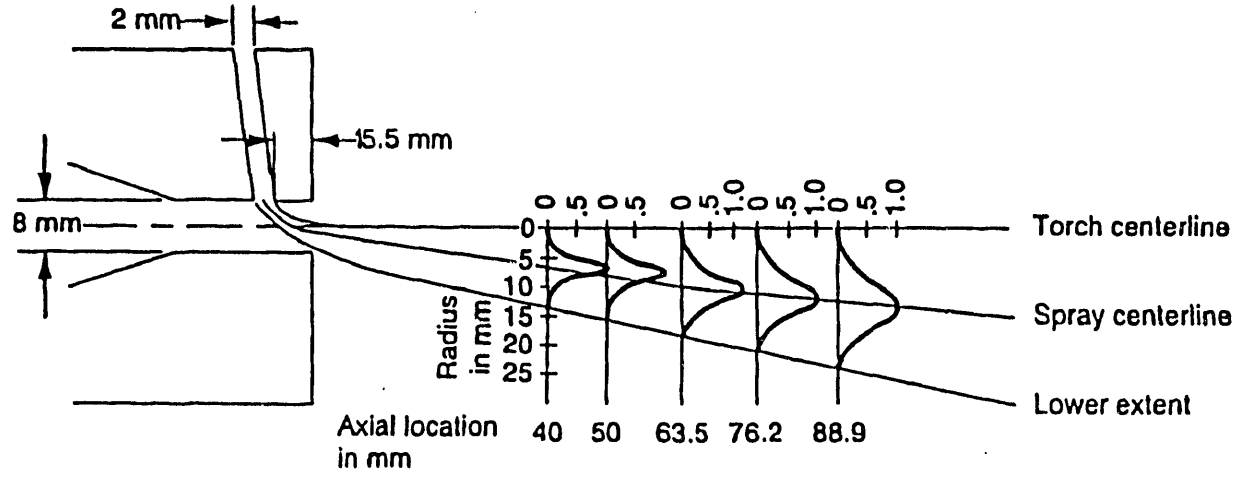

FIG. 1.Plasma torch geometry with normalized particle number density distribution.

available.

At an axial location 5 mm from the face of the torch and on its geometric center line the gas temperature was determined to be approximately 12700 K. At this close proximity to the exit, the gradients are steep, and the temperature drops off rapidly to 2000 K at the 5 mm radial location which is just outside of the 8 mm nozzle exit diameter. The maximum velocity measured is approximately 1300 m/s near the center line at the 5 mm axial location. The corresponding Mach number is .47 which is slightly above the normal compressible limit of .3 but not high enough to introduce significant errors when using the Bernouli equation to calculate velocity from the measured stagnation pressure.

Particle parameters have been investigated between axial locations of 40 and 110 mm. The measured particle temperatures are in excess of the 1900 K melting point of high nickel content Ni-Al alloys. Average Particle velocities range from approximately 180 m/s on the torch centerline to 80 m/s in the periphery of the jet. The particle/gas interactions were investigated by overlaying the particle and gas flow field measurement data.

As shown earlier, the particle flow field is characterized by an asymmetric trajectory, i.e. the majority of particles fly through the plasma jet and exit the opposite side of the gas flow field. Therefore when considering the environment which an average particle experiences, one must follow the median trajectory of the particle spray field. Figure 2, 3, and 4 are contour plots of the gas flow field temperature, velocity, and percent air concentration, respectively, with the dashed line indicating the median trajectory. The zero axial position is the exit of the torch and the particles are injected 15 mm upstream of the torch exit. The temperature map shows that the majority of particles do not travel through the hottest portion of the plasma. Particles traveling on the centerline of the plasma plume do not see temperatures below 3000 K until the 55 mm axial position and those traveling on the particle flow field centerline experience temperatures below 3000 K by the 20 mm axial position. The implications here are that the average particle begins to transfer heat back to the gas sooner than if it followed the center line of the plasma. This is verified in Figure 5, which is a plot of average particle temperature and the gas temperature along the median particle trajectory. The slight downward trend of average particle temperature is consistent with the trend of lower gas temperatures as one moves outward both axially and radially. A typical radial distribution of gas and particle temperature for the 63.5 mm axial position is shown in Figure 6. Particles on the centerline are generally hotter because they have been exposed to higher temperatures and are smaller than those on the periphery of the spray field. A similar scenario is observed in the measured velocities, Figure 3. While

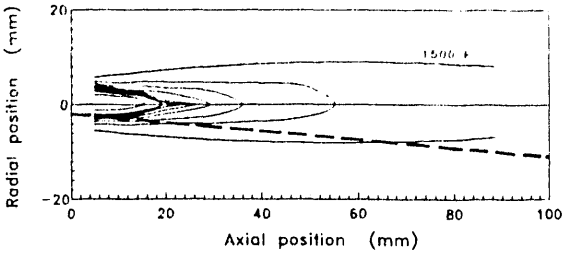

FIG. 2. Contour plot of gas temperature with the highest particle number density shown by the dashed line. Contours are in increments of 1500 K.

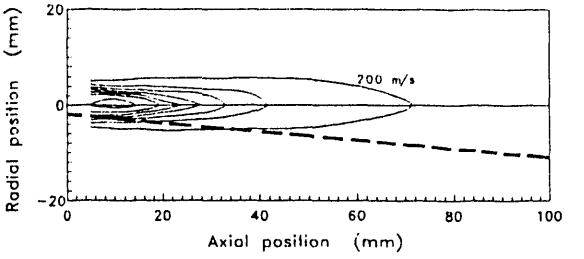

FIG. 3. Contour plot of gas axial velocity with the highest particle number density shown by the dashed line. Contours are in increments of 200 m/s.

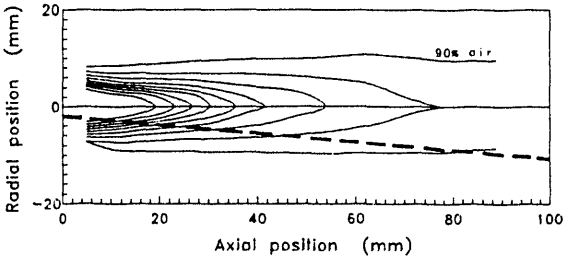

FIG. 4. Contour plot of air concentration with the highest particle number density shown by the dashed line. Contours are in increments of 10%.

the 200 m/s contour extends to over 70 mm on the plasma center line, the average particle experiences a gas velocity of less than 200 m/s by the 30 mm axial location. The cross over point of particle and gas axial velocities along the median trajectory of the particles is shown in Figure 7. The average particle is accelerated by the gas, out to approximately 60 mm from the face of the torch

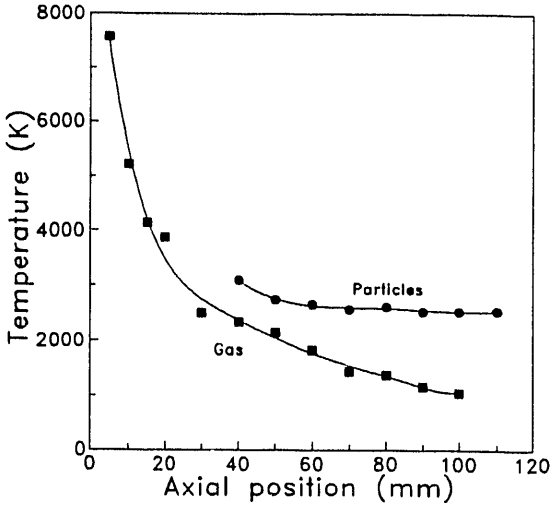

FIG. 5. Gas and particle temperatures on the median particle trajectory.

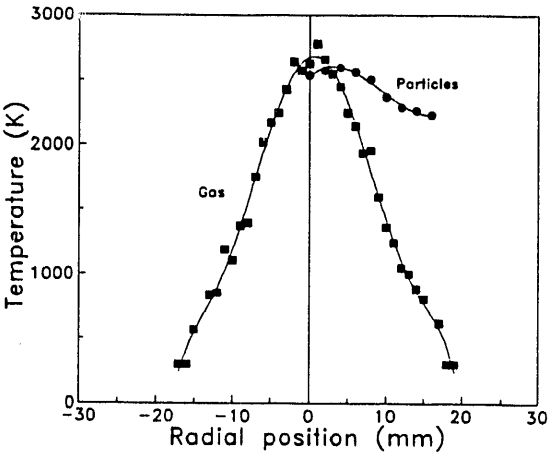

FIG. 6. Radial distribution of particle and gas temperature at the 63.5 mm axial position.

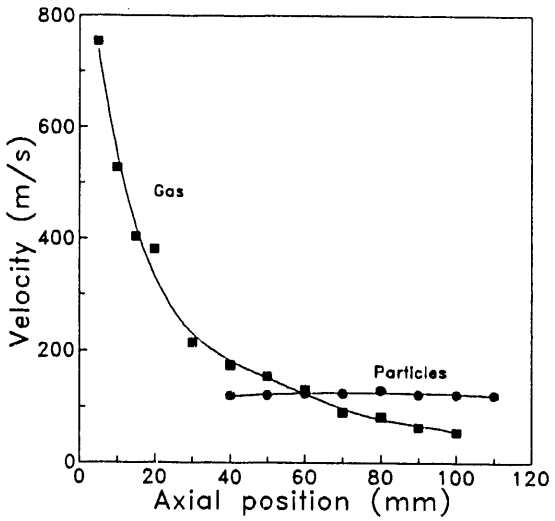

FIG. 7. Axial velocity of gas and particles along the particle trajectory center line.

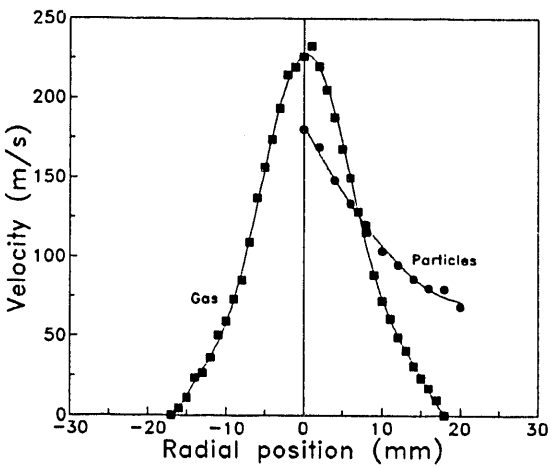

FIG. 8. Radial distribution of average particle and gas axial velocity at the 63.5 mm axial position.

where the gas and particle velocities match. Further out the particle has a higher velocity than the gas and therefore is retarded by the surrounding gas. A typical radial distribution of axial velocity for both the gas and particles at the 63.5 mm axial location is shown in Figure 8. Again due to their smaller size and longer exposure to a higher velocity difference it is expected that the particles on the gas jet centerline would have a higher velocity than those in the periphery.

Conclusions

In-flight particle parameter data (particle size, velocity, temperature, and number density) in combination with maps of the gas flow field provides information on the history and environment of an average particle as it travels to the substrate. Due to the asymmetry of the particle flow field an average particle on the median trajectory experiences lower gas temperatures and accelerating forces than does a particle which follows the centerline of the plasma plume. By the time an average particle reaches the nominal substrate standoff it is being cooled and decelerated by the plasma gas. Combining the flow field maps in this way makes it possible to optimize the median particle trajectory for the desired average particle conditions, i.e. temperature and velocity, at the substrate. Data of this type is also useful in bench

marking and developing physically accurate models describing the spray coating process. The result is, greater insight into the important parameters of the process and ultimately, better control of the coating quality.

Acknowledgements

This work was supported by the U.S. Department of Energy, Assistant Secretary for Energy, Office of Basic Energy Sciences, and Laboratory Directed Research and Development funds under DOE Contract No. DE-AC07-76ID01570.

References

1. S. C. Snyder and L. D. Reynolds, "Measurement of Thermal Plasma Jet Temperature and Velocity by Laser Light Lineshape Analysis," Proceedings of the International Conference on Phenomena in Ionized Gases, 1991, Barga, Italy

2. J. R. Fincke, R. Rodriguez, and C. G. Pentecost, "Coherent Anti-Stokes Raman Spectroscopic Measurement of Air Entrainment in Argon Plasma Jets," Plasma Processing and Synthesis of Materials III, Materials Research Society Symposia Proceedings Vol. 190, April 1990, San Francisco, CA

3. J. R. Fincke, R. Rodriguez, and C. G. Pentecost, "Measurement of Air Entrainment in Plasma Jets," Proceedings of the 1990 National Thermal Spray Conference, Long Beach, CA, pp. 45-48, May 1990

4. Grey, J., "Thermodynamic Methods of High-Temperature Measurement", ISA Transactions, Vol. 4, No. 2, 1965

5. Katta, S., J. A. Lewis, and W. H. Galvin, "A Plasma Calorimetric Probe", Rev. Sci. Instrum., Vol. 44, No. 10, 1973

6. Grey, J., P.F. Jacobs, and M.P. Sherman, "Calorimetric Probe for the Measurement of Extremely High Temperatures", Review of Scientific Instruments, Vol. 33 (7), July 1962

7. Chen, W.L.T., J. Heberlein, and E. Pfender, "Experimental Measurements of Plasma Properties for Miller SG-100 torch with Mach I Settings. Part 1: Enthalpy Probe Measurements", Report, Engineering Research Center for Plasma-Aided Manufacturing, Dept. of Mech. Engr., Univ. of Minn. August 1990

8. Brossa, M., E. Pfender, "Probe Measurements in Thermal Plasma Jets", Plasma Chem. Plasma Process., 8, 75 (1988)

9. Capetti, A., E. Pfender, "Probe Measurements in Argon Plasma Jets Operated in Ambient Argon", Plasma Chem. Plasma Process., 9, 329 (1989)

10. Fincke, J.R., W.D. Swank, and C.L. Jeffery, "Simultaneous Measurement of Particle Size, Temperature and Velocity in Thermal Plasmas", IEEE Trans. on Plasma Sci., PS-18 948 (1990)

11. Swank, W.D, J.R. Fincke, and D.C. Haggard, "Modular Enthalpy Probe and Gas Analyzer for Thermal Plasma Measurements", accepted for publication in Review of Scientific Instruments

12. Gordon, S. and B. McBride, "Computer Program for Calculation of Complex Chemical Equilibrium Compositions, Rocket Performance, Incident and Reflected Shocks, and Chapman-Jouguet Detonations",NASA SP-273, Lewis Research Center, 1976)

13. Kline, S. J., and F. A. McClintock, "Describing Uncertainties in Single- sample Experiments, Mech. Eng., P.3, January 1953

14. Fincke, J.R. and W.D. Swank, "Simultaneous Measurements of Ni-Al Particle Size, Velocity, and Temperature in Atmospheric Thermal Plasmas", Proceedings of the 3rd National Thermal Spray Conference, Long Beach, CA, May 1990

15. Vardelle, A., M. Vardelle, P. Fauchais, P. Proulx and M. I. Boulos, "Loading Effect by Oxide Powders in DC Plasma Jets", Proc. of the Intenational Thermal Spray Conference, Orlando, 543 (1992)

16. Chang, C.H., "Numerical Simulation of Alumina Spraying in an Argon-Helium Plasma Jet", Proc. of the Intenational Thermal Spray Conference, Orlando, 793 (1992)

END

DATE
FILMED
6/9/93